Temporally dynamic photopolymerization of C_{60} molecules encapsulated in single-walled carbon nanotubes

Yuika Saito,[1] Mitsuhiro Honda,[2] Yoshikiyo Moriguchi,[2] and Prabhat Verma[2,*]

[1]*Frontier Research Center, Osaka University, 2-1 Yamadaoka, Suita, Osaka 565-0871, Japan*
[2]*Department of Applied Physics, Osaka University, Yamadaoka 2-1, Suita, Osaka 565-0871, Japan*

The photopolymerization of carbon-60 (C_{60}) molecules encapsulated inside single-walled carbon nanotube (*en*-C_{60}) is investigated through far-field and near-field Raman spectroscopies. In general, a moderately intense laser irradiation invokes complete photopolymerization of nonencapsulated bulk C_{60} molecules (bulk-C_{60}). However, in contrast, we observed in our experiments that the *en*-C_{60} molecules never get completely polymerized, even under long and strong irradiation. In both far-field and near-field Raman measurements, we observed evidences of simultaneous occurrence of polymerization and depolymerization of *en*-C_{60} during the process of irradiation. The temporal fluctuation of Raman intensity associated with C_{60}-monomer peak confirmed that *en*-C_{60} molecules jump back and forth between the polymerized and depolymerized states. The results have been discussed through the unique movement of C_{60} molecules inside nanotube, and through the interaction between C_{60} molecules with the inner wall of the nanotube in *en*-C_{60} sample, which generates frictional heat, responsible for the scission of polymeric bonds between neighboring C_{60} molecules. The frictional scission competes with the photopolymerization process, resulting in a temporally dynamic situation where the sample can never get completely polymerized even under strong irradiation.

I. INTRODUCTION

Since the discovery of carbon-60 (C_{60}) in 1985, it has been one of the most investigated molecules of its family,[1] because this molecule in its composite nanostructural form has promising characteristic for future nanoscale devices by controlling the shapes and the chemical properties of the composite.[2–4] Indeed C_{60} acts as a strong acceptor upon photo excitation and can be used for photoconductor, light-emitting diode,[5] second-order nonlinear optical material,[6] and optical limiting devices.[7] One of the interesting features of C_{60} is that it is known to polymerize under UV to visible light irradiations, forming a variety of crystal structures such as rhombohedral, tetragonal, or orthorhombic, depending upon the polymerization conditions.[8,9] In fact, it is believed that the photochemical process in C_{60} is very efficient, leading to one dimmer per absorbed photon.[10] It is also reported that C_{60} could be efficiently encapsulated in a quasi-one-dimensional single-walled carbon nanotube (SWNT),[11] which can lead to interesting applications. Photopolymerization process of C_{60} encapsulated in SWNT (*en*-C_{60}) has also been investigated in the recent past,[12–14] where the possibility of C_{60} partially forming a one-dimensional chain was suggested. The polymerization process was monitored through the decreasing intensity of Raman peak that corresponds to isolated C_{60} molecules (monomers). The authors could not confirm complete polymerization in their experiment, as the Raman peak corresponding to the monomers never disappeared completely. Nevertheless, they concluded that at sufficiently high laser irradiation, the C_{60} molecules would completely polymerize and would form a perfect one-dimensional chain inside the SWNT. The sample used in their study was extremely dense, where it is difficult to understand the flow of energy during the laser irradiation. In contrast, in a thorough study, we have found that under am-

bient conditions it is impossible for *en*-C_{60} molecules to completely polymerize, even under a long-time high-power laser irradiation reaching the threshold of ablation, for a sample that is fairly dispersed. It should be noted here that even if the SWNTs are dispersed, we have confirmed that the intermolecular distance for these *en*-C_{60} molecules inside a SWNT is short enough for a possible polymerization to take place. Instead, we found evidences of random events of polymerization and depolymerization during a long exposure, which never leads to a complete polymerization with formations of one-dimensional C_{60} chain inside the SWNT. Our results are also in contrast to some of the XRD observations[15–17] where authors demonstrated reduced intermolecular distances confirming complete polymerization of C_{60} molecules inside SWNT. However, this was observed only under high pressure and high temperature, which is completely different experimental environment in comparison with the present report under atmospheric pressure and room temperature.

Out of several Raman-active vibrational modes of C_{60} molecules, only the nondegenerate $A_g(2)$ pentagonal pinch mode at 1467 cm^{-1} is strong enough to be detectable from a small volume of the sample. When C_{60} monomer molecules turn into oligomers, they create covalent bindings resulting in complexity in Raman spectrum. The most distinguished change due to this covalent bonding appears in the $A_g(2)$ mode, which lowers its vibrational frequency by about 10 cm^{-1}, easily detectable in Raman spectra. Therefore, a comparison of the intensity ratio between the monomer and oligomer peaks can provide a quantitative measure for the amount of polymerization. In the case of complete polymerization, the monomer peak would disappear. Thus, it is very convenient to utilize Raman spectroscopy to study the polymerization phenomenon in C_{60} molecules.

Apart from overcoming an energy barrier for the process of polymerization to occur, it is also required that the C_{60}

molecules align parallel to the reactive carbon double bonds of the adjacent molecules and stay in close proximity for the 2+2 cycloaddition covalent bonding to take place. In fact, under room temperature, C_{60} molecules freely spin along randomly oriented axis, which gives them a possibility to change their relative orientations. When excited with external light, the long-lived triplet state of C_{60} gives the molecules enough time to orient parallel during their random spin and to form polymeric covalent bonds with the neighboring molecules, provided the molecules are in close proximity.[18] Thus, photopolymerization of C_{60} can readily occur under sufficiently intense light irradiation. On the other hand, it is also known that the polymeric covalent carbon double bonds in an oligomer can easily break to create monomers, if sufficient energy is provided to the oligomers, for example, by means of raising the temperature.[19] This means, while C_{60} monomers could be polymerized by light, they can also return back to the monomer state under the presence of sufficient energy. Thus, if there is another source of energy, the C_{60} molecules under light irradiation may undergo a temporal fluctuation of phase between monomer and oligomer. This is what we have observed in the case of *en*-C_{60} molecules, and we anticipate that this behavior is associated with the unique movement of *en*-C_{60} molecules, which receives enough energy from the surrounding SWNT to overcome the energy barrier to jump back and forth between polymerized and depolymerized states.

In this paper, we report on the photopolymerization phenomena of *en*-C_{60} molecules, measured through confocal micro-Raman spectroscopy. In order to compare the photopolymerization process of *en*-C_{60} molecules with that of free C_{60} molecules, we have also studied the process of photopolymerization of C_{60} molecules dispersed uniformly on a glass substrate, which we refer as the bulk-C_{60} sample. By changing the irradiation power and the exposure time, we monitored the relative strengths of Raman peaks that correspond to the monomers and oligomers of C_{60} molecules, to understand the process of polymerization. Further, we have also analyzed the sample through the technique of tip-enhanced Raman spectroscopy (TERS) (Refs. [20–23]) that allows us to selectively study nanometric area of the sample. The results on photopolymerization of *en*-C_{60} molecules are discussed through the spectroscopic signatures of polymerization and depolymerization.

II. EXPERIMENTAL DETAILS

The C_{60} molecules and the SWNTs used in this study were purchased from Matsubo Co. and Meijo Carbon Co., respectively. For the preparation of bulk-C_{60} sample, 8.3 mM of C_{60}-toluene solution was dropped on a cover-glass slip and dried at the temperature of 180 °C. The sample was dried at a fast rate so that a possible crystallization and formation of isotropic sample could be avoided. In order to prepare *en*-C_{60} sample, SWNTs were sonicated in nitric acid solution for 6 h to open the tube ends. The open-ended SWNTs were evacuated in a quarts glass cell for 30 min at the temperature of 400 °C for perfect drying. The SWNTs were then mixed with C_{60} molecules and the mixture was

heated to 600 °C for 12 h after sealing them in a quartz-glass cell under a pressure of $\sim 10^{-5}$ torr. The mixture was then dissolved in toluene and was sonicated followed by the filtration to remove extra C_{60} molecules outside of the tube.[24] The purification process was repeated several times to completely remove the unencapsulated C_{60} molecules. The filtrated C_{60}-SWNT was dispersed in 2,2,3,3-tetrafluoro-1-propanol and drop-and-dry coated on a cover-glass slip for Raman measurements. Encapsulation was confirmed by both Raman spectroscopy and transmission electron microscope (TEM) imaging.

Utilizing a 532-nm diode laser, the sample was illuminated and confocal Raman scattered light was collected through a high-numerical-aperture (NA) objective lens. The collected Raman signal was dispersed through a polychrometer and the dispersed signal was recorded by a liquid-nitrogen-cooled charge coupled device (CCD) camera. In order to invoke photopolymerization, the sample was exposed to various values of illumination power, however, Raman scattering was always excited by a low laser power of 8 μW, which we confirmed to be too low for causing any structural changes, including polymerization, even for a long exposure of more than 100 min. All the experiments were carried out under room temperature.

For TERS measurements, the sample was excited with 400 μW of a 488-nm diode laser. The beam was expanded 20-fold using a beam expander and an evanescent mask was inserted in the beam path. A cover-glass slip, on which the sample was placed, was set on an inverted oil-immersion microscope objective lens ($\times 60$, NA=1.4). The Raman signal was efficiently collected by the same objective lens. A pinhole with a diameter of 200 μm was inserted in the collection path to decrease the intensity of background far-field signal. The collected signal was guided to a single spectrometer and detected using a liquid-nitrogen-cooled CCD camera. TERS was excited by bringing a metallic nanotip close to the sample. The nanotip was prepared by coating silver on a commercially available AFM cantilever by vacuum evaporation that resulted in a tip with apex diameter of about 30 nm. The reference data was collected by taking the tip off the sample.

III. RESULTS AND DISCUSSION

Electron microscopy is one of the common ways to image nanomaterials. We therefore utilized this technique for the preliminary visualization of the encapsulation of C_{60} molecules in SWNTs. The TEM image of *en*-C_{60} sample, an example of which is shown in Fig. 1, confirms that there were no C_{60} molecules attached on the outer walls of the SWNTs or anywhere between the SWNTs. This was also confirmed by taking the TEM image from different parts of the sample. A careful observation of the contrast in TEM image indicates the presence of C_{60} molecules inside the nanotubes, which was further confirmed from x-ray diffraction and Raman scattering to compliment the TEM image. It can also be observed in this image that C_{60} molecules are in physical contact, indicating the possibility of one-dimensional polymerization of C_{60} molecules inside the
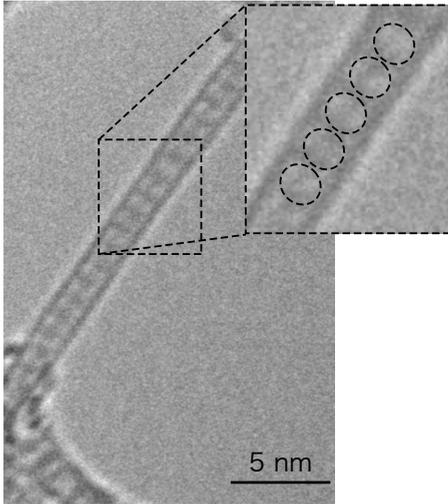
FIG. 1. TEM image of C_{60} encapsulated in an isolated SWNT. The contrast in this image depicts the presence of closely packed C_{60} molecules inside the tube, as illustrated by the dotted circles in a zoomed area in the inset. This is also evident that there are no C_{60} molecules on the outer wall of the SWNT.

SWNT. We also confirmed the amorphous nature of bulk-C_{60} sample through scanning electron microscope (SEM) images (not shown here), which suits better for photopolymerization process in comparison with crystalline samples.

A. Photopolymerization of bulk-C_{60}

In order to understand the process of photopolymerization in *en*-C_{60}, we first investigated the bulk-C_{60} sample by studying the power dependence of laser irradiation on the photopolymerization process. Figure 2 shows Raman signature on the photopolymerization of bulk-C_{60} probed through the $A_g(2)$ pentagonal pinch mode.[3] Raman spectra of bulk-C_{60} before and after laser irradiation ($\lambda = 532$ nm, power $= 1$ mW, and exposure $= 1$ min) are shown in Fig. 2(a). Before laser irradiation, Raman spectrum shows the $A_g(2)$ mode at 1467 cm^{-1}, which corresponds to monomer C_{60} molecules. This peak is suppressed after laser irradiation and a new peak appeared at 1457 cm^{-1}, which corresponds to the vibrational mode of percolating clusters of molecules caused by polymerization process. This mode was originally a tangential $A_g(2)$ symmetry mode in pristine C_{60}.[25] Figure 2(b) shows the power dependence of the laser irradiation for the photopolymerization process, which is quantified by the intensity ratio of I_{1467}/I_{1457}, where I_{1467} and I_{1457} represent Raman intensities of the monomer mode at 1467 cm^{-1} and the polymer mode at 1457 cm^{-1}. The irradiation wavelength was 532 nm, the illumination power was varied from 0 to 1 mW and the sample was exposed for 1 min in every experiment. The laser power during Raman measurements was set to 8 μw and Raman signal was accumulated for 5 min. In order to polymerize a fresh area of the sample, each experiment was performed at different positions of the sample, however, we confirmed by SEM image that the sample was uniform within the microscopic observation area. As one can clearly see from Fig. 2(b), the irradiation power significantly
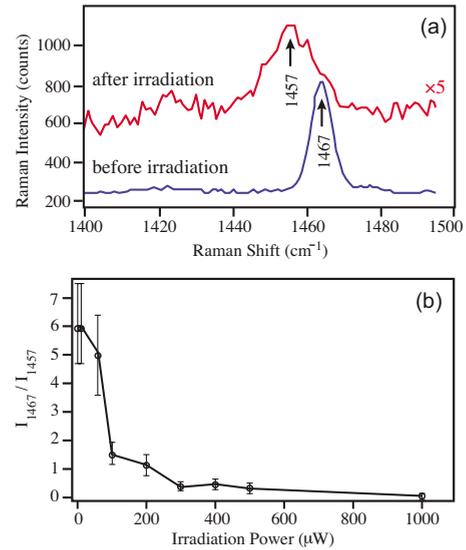

FIG. 2. (Color online) (a) Raman spectra of bulk-C_{60} sample in the spectral range of $A_g(2)$ mode, before (lower curve) and after (upper curve) laser irradiation. The blue spectrum shows a monomer peak at 1467 cm^{-1} while the red spectrum shows a polymer peak 1457 cm^{-1}. (b) Laser irradiation power dependence of the amount of polymerization, quantified by the intensity ratio I_{1467}/I_{1457}, where I_{1467} and I_{1457} represent Raman intensities of the modes at 1467 and 1457 cm^{-1}, respectively. The exposure time, the accumulation time and the observation laser power for Raman measurements were 1 min, 5 min, and 8 μW, respectively.

affects the degree of photopolymerization. The threshold irradiation power necessary for photopolymerization of bulk-C_{60} is about 80 μw and the irradiation power of about 200 μw is enough to cause complete photopolymerization within 1-min exposure.

B. Photopolymerization of *en*-C_{60}

The presence of SWNT surrounding in encapsulated sample significantly changes the photopolymerization behavior of *en*-C_{60} in comparison with that of bulk-C_{60} under ambient conditions. Unlike the bulk-C_{60} sample, the *en*-C_{60} sample does not show complete polymerization even after stronger and longer exposures. This is evident from the presence of monomer peak in Raman spectrum, which always appears with noticeable intensity. Figure 3(a) shows two Raman spectra obtained at two different excitation powers and accumulation time from the *en*-C_{60} sample. The lower spectrum in Fig. 3(a) was obtained with 8 μW of excitation and 100 min of accumulation, which we confirmed to be too low to invoke photopolymerization while the upper spectrum was obtained with 500 μW of excitation and 5 min of exposure, which is high enough to cause a thorough photopolymerization in bulk-C_{60}. In order to focus our attention on vibrational mode associated with C_{60}, the spectra are corrected for SWNT background and are shown in the spectral range of 1450–1480 cm^{-1}. The blue spectrum shows a peak at 1464 cm^{-1}, which is downshifted by 3 cm^{-1}, in comparison with the $A_g(2)$ mode of bulk-C_{60}. This shift originates from the interaction between the SWNT wall and C_{60} molecules,
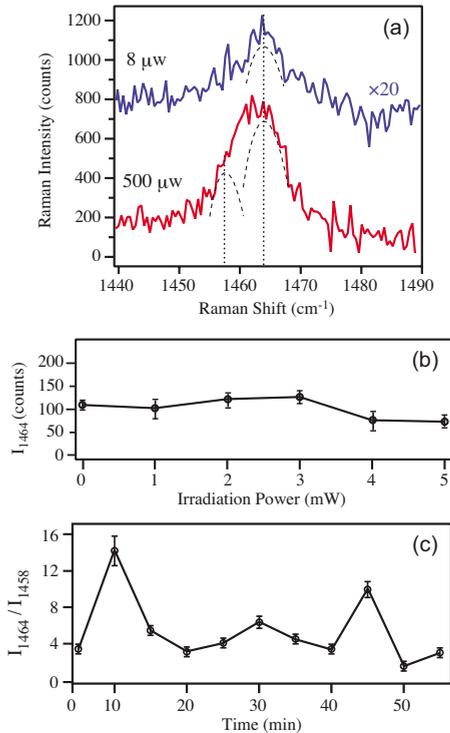
FIG. 3. (Color online) (a) Raman spectra of *en*-C_{60} sample in the spectral range of $A_g(2)$ mode, measured with two different observation laser powers of 8 μW (blue curve) and 500 μW (red curve). In order to focus our attention on the C_{60} vibrational modes, the SWNT background signal was removed. The $A_g(2)$ mode in blue spectrum is observed at 1464 cm^{-1}, which is downshifted by 3 cm^{-1} in comparison with bulk-C_{60} sample due to encapsulation. This peak is still observed in the red spectrum, which, in addition, shows a polymer peak at 1458 cm^{-1}, as illustrated by the dotted curves. (b) Irradiation power dependence of the monomer peak intensity. The exposure time, the accumulation time and the observation laser power were 1 min, 20 min, and 8 μW, respectively. (c) Time dependence of the intensity ratio I_{1464}/I_{1458}, where I_{1464} and I_{1458} represent Raman intensities of the modes at 1464 and 1458 cm^{-1}, respectively. All measurements were performed under 500 μW irradiation with an accumulation time of 5 min from the same spot of the sample.

and is characteristic of the encapsulation.[26] On the other hand, the red spectrum shows a broader peak, which can be deconvoluted into two modes appearing at 1458 and 1464 cm^{-1}. It is interesting to see that the peak at 1464 cm^{-1} still appears with noticeable intensity, indicating that, unlike in the bulk-C_{60} sample, C_{60} monomers still exist in the *en*-C_{60} sample at such a strong exposure. The other peak at 1458 cm^{-1} comes from C_{60} oligomers, indicating the coexistence of polymerized and unpolymerized sample during the measurement time.

Focusing our attention to the monomer peak at 1464 cm^{-1}, we measured the intensity of this peak after 1-min exposure with various irradiation powers, which is shown in Fig. 3(b). Each spectrum was measured with 8 μW of excitation power for an accumulation time of 20 min from a fresh area of the sample and the intensity of C_{60} mode was calibrated with the intensity of the *G* band of

SWNT to avoid any possible inhomogeneity of the sample. The irradiation power was varied from 0 to 5 mW. For irradiation power larger than 5 mw, the sample started to get damaged due to the effect of laser ablation. As can be noticed from Fig. 3(b), the intensity of $A_g(2)$ mode does not show any obvious dependence on the irradiation power, which is very different from what we saw in the case of bulk-C_{60} sample in Fig. 2(b). This indicates that the C_{60} monomers still exist and their average amount remains unchanged even around the threshold irradiation power that causes ablation of the sample. It was confirmed from x-ray diffraction that average intermolecular distance of C_{60} encapsulated in SWNT was shorter than that of monomers but longer than that of the polymer,[9,13] which means C_{60} molecules were close enough to form polymer under light irradiation.

A closer look at the experimental results, however, indicated that the flat response of Raman intensity in Fig. 3(b) was averaged over the exposure time. Indeed, we found that the Raman intensity of the $A_g(2)$ mode fluctuates randomly over a period of time. Figure 3(c) shows the time dependence of the intensity ratio between the polymer and monomer peaks of *en*-C_{60} sample. Raman spectra were measured from the same area of the sample with an accumulation time of 5 min and an excitation power of 500 μw, which showed visible fluctuation of Raman intensities over the time. The fluctuation of the intensity ratio in Fig. 3(c) clearly indicates that there is a temporal dynamic phase change of *en*-C_{60} between polymer and monomer during the light exposure. It should also be noted that we could not see any temporal fluctuation in the $A_g(2)$ mode under the exposure of 8 μW, confirming that the temporal fluctuation in Fig. 3(c) was evoked by the strong irradiation.

The spatial resolution in above-mentioned experiments was about 500 nm and hence the temporal fluctuation observed in Fig. 3(c) was also averaged over the focal area in Raman measurements. In order to understand this temporal fluctuation at a much higher spatial resolution, we utilized the TERS technique, where the observation area is comparable to the size of the tip apex ($\sim$30 nm in present case). Thus, by utilizing TERS, we could study the temporal fluctuation from a much smaller area of the sample. Figure 4(a) shows TERS spectra from *en*-C_{60} sample, where the red spectrum was measure with tip in close contact with the sample while the reference far-field spectrum in blue was measured by taking the tip off the sample. Due to the lower sensitivity in TERS experiments, one can hardly see the $A_g(2)$ mode of C_{60} in the far-field spectrum shown in blue. However, as the tip comes close to the sample, the enhanced spectrum, presented in red, clearly shows the $A_g(2)$ mode of C_{60}, which originated from a very small volume in close vicinity of the tip apex. It was found that the $A_g(2)$ mode in TERS spectrum shows much faster temporal fluctuation, in comparison with the previous case of far-field measurements in Fig. 3. Figure 4(b) shows the intensity fluctuation in $A_g(2)$ mode in TERS, measured from the same area of the sample at intervals of 2 min. Here, instead of the intensity ration between the monomer and polymer peaks, we plot only the intensity of the monomer peak, because the signal-to-noise ratio for the polymer peak was significantly weak in TERS measurements. The temporal fluctuation in Raman intensity
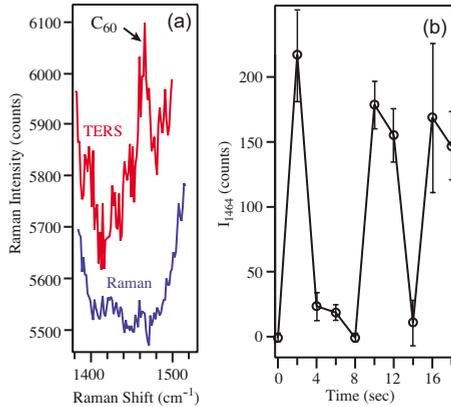
FIG. 4. (Color online) (a) Near-field Raman spectra of *en*-C_{60} sample in the spectral range of $A_g(2)$ mode. Blue curve shows normal Raman spectrum (far-field) while the red curve shows TERS spectrum (near-field). Due to poor sensitivity in these experiments, the $A_g(2)$ mode cannot be observed in the far-field, however, it appears clearly in the TERS spectrum due to the field enhancement. (b) Time dependence of TERS intensity of the monomer peak at 1464 cm^{-1} obtained from a fixed sample position. The spectra were recorded under 400 μW observation power with accumulation time of 2 s. The temporal fluctuation of this peak becomes stronger and frequent when measured from a small area ($\sim$30 nm) of the sample in TERS experiments.

in Fig. 4(b) clearly indicates that the C_{60} molecules encapsulated in SWNT jump back and forth between the monomer and polymer phase under light irradiation. This is more clearly seen from a smaller volume of the sample, where there are lesser possibilities of averaged observations. Also, TERS results show a faster fluctuation than the far-field measurements, because, owing to the field enhancement, TERS has the capabilities of faster measurements.

The temporal fluctuation of Raman intensity is a clear evidence of the fact that under sufficient light irradiation, the C_{60} molecules in *en*-C_{60} sample jump back and forth between polymer and monomer phases. A similar situation could not be observed in the case of bulk-C_{60}, which means this phenomenon is somehow related to the encapsulation. While, in the process of polymerization, new C-C bonding between neighboring C_{60} molecules is established through the irradiation, simultaneous scission of these bonds take place due to the interaction of C_{60} molecules with SWNT, which brings the molecules back into monomer phase. Thermal vibration is one of the known driving forces for the scission of polymeric bonds. It has been observed that even by the heat created by the irradiation laser, C-C polymeric bonding can break.[19] In such situation, bond forming competes with thermal scission in the same experiment. In our case, apart from the laser heating, the thermal energy comes from the interaction between *en*-C_{60} molecules and the inner wall of SWNT, mostly as friction. It is known that C_{60} molecules can rotate freely inside the SWNT at room temperature.[27–29] In a recent study through NMR,[28] it was observed that the free rotation of C_{60} molecules brings in some interference from the inner walls of the SWNT preventing the polymerization of C_{60} molecules inside the nanotube. Another study through neutron scattering[29] depicted

strong orientational disorder due to the rotations of C_{60} molecules. In both reports, the authors observed that the rotation of C_{60} molecules invokes some interaction between C_{60} molecules and the inner walls of SWNT, which interferes with the polymerization process. We believe this interaction is the frictional force that generates some heat, which helps in breaking up the C_{60}-C_{60} bondings. Similarly, a short oligomer can rotate along the axis of the SWNT. In this situation, the friction force between C_{60} molecule and the inner wall of SWNT would twist the polymer chain, making it possible to break the polymeric bond. In addition, C_{60} molecules in *en*-C_{60} sample can also move back and forth inside SWNT because of the inner force called internal pressure.[30] Internal pressure is a static capillary force between C_{60} molecules and the inner wall of SWNT, which is considered as the driving force for the encapsulation.[31] Friction is also created by this internal pressure, which can lead to the scission process of C_{60} polymer inside SWNT. Indeed, in a high-resolution TEM imaging experiment,[32] it was observed that C_{60} molecules formed bonds with SWNT walls under electron beam irradiation and few seconds later, the bonds recovered. The author claimed that such coalescence was not a particular phenomenon under the electron-beam irradiation but can be more generally found in a study with careful heat treatments. Such bond formation would also change the bonding energy of the original polymeric bonds, helping the scission process to occur easier than the case of bulk-C_{60}. It can easily be predicted that such bond formation would also act as a friction force for the inner movement of C_{60} molecules, leading to the scission process. Thus we conclude that the interaction between C_{60} molecules and the inner wall of SWNT is the driving force of the scission, which competes with the polymeric bond formation under light irradiation. We also note here that polymer bond breaking was not reported to occur in the experiments where polymerization of encapsulated C_{60} molecules was seen under high pressure and high temperature,[15–17] even after returning back to the ambient conditions. This means that our observation of spontaneous polymer bond breaking at ambient condition is somehow also related to high laser irradiation. We believe that the laser irradiation adds further energy to the frictional heat, resulting in easy scission of the polymer bonds. Due to this dynamic situation, the *en*-C_{60} molecules never form a steady one-dimensional polymer inside the SWNT, even though their intermolecular distances are short enough for the polymerization to take place. Rather, they jump back and forth between monomer and polymer states with time, the signature of which can be found in the form of temporal fluctuation of Raman intensities.

IV. CONCLUSIONS

In conclusion, the laser-irradiated photopolymerization process of encapsulated C_{60} molecules inside SWNTs was investigated through Raman and TERS measurements. Unlike the nonencapsulated bulk-C_{60} molecules, we observed that the *en*-C_{60} molecules never get completely polymerized, even under long and strong irradiation. Both Raman and

TERS measurements showed evidences of simultaneous occurrence of polymerization and depolymerization of *en*-C_{60} during the laser irradiation. The unique movement of C_{60} molecules inside SWNT generates frictional heat, which results in the scission of polymeric bonds between neighboring C_{60} molecules. Thus, heat-generated polymeric bond breaking competes with photogenerated polymerization process during the laser irradiation, resulting in a dynamic coexistence of polymers and monomers. This phenomenon is observed through the temporal fluctuation of Raman intensity associated with C_{60}-monomer peak, which confirmed that *en*-C_{60} molecules jump back and forth between the polymerized and depolymerized states during laser irradiation.

*verma@ap.eng.osaka-u.ac.jp

[1] H. W. Kroto, J. R. Heath, S. C. O'Brien, R. F. Curl, and R. E. Smalley, Nature (London) **318**, 162 (1985).

[2] Y. Liu, S. C. O'Brien, Q. Zhang, J. R. Heath, F. K. Tittel, R. F. Curl, H. W. Kroto, and R. E. Smalley, Chem. Phys. Lett. **126**, 215 (1986).

[3] M. S. Dresselhaus, G. Dresselhaus, and P. C. Eklund, *Science of Fullerenes and Carbon Nanotubes* (Academic Press, San Diego, 1996).

[4] F. Diederich, L. Isaacs, and D. Philp, Chem. Soc. Rev. **23**, 243 (1994).

[5] L. W. Tutt and T. F. Boggess, Prog. Quantum Electron. **17**, 299 (1993).

[6] C. A. Mirkin and W. B. Caldwell, Tetrahedron **52**, 5113 (1996).

[7] N. S. Sariciftci, Prog. Quantum Electron. **19**, 131 (1995).

[8] A. M. Rao *et al.*, Science **259**, 955 (1993).

[9] A. M. Rao, P. C. Eklund, J-L. Hodeau, L. Marques, and M. Nunez-Regueiro, Phys. Rev. B **55**, 4766 (1997).

[10] Y. Wang, J. M. Holden, Z. H. Dong, X. X. Bib, and P. C. Eklund, Chem. Phys. Lett. **211**, 341 (1993).

[11] H. Kataura, Y. Maniwa, T. Kodama, K. Kikuchi, K. Hirahara, K. Suenaga, S. Iijima, S. Suzuki, Y. Achiba, and W. Krätschmer, Synth. Met. **121**, 1195 (2001).

[12] T. Pichler, H. Kuzmany, H. Kataura, and Y. Achiba, Phys. Rev. Lett. **87**, 267401 (2001).

[13] H. Kataura, Y. Maniwa, M. Abe, A. Fujiwara, T. Kodama, K. Kikuchi, H. Imahori, Y. Misaki, S. Suzuki, and Y. Achiba, Appl. Phys. A: Mater. Sci. Process. **74**, 349 (2002).

[14] F. Cui, C. Luo, and J. Dong, Phys. Lett. A **327**, 55 (2004).

[15] M. Chorro, S. Rols, J. Cambedouzou, L. Alvarez, R. Almairac, J.-L. Sauvajol, J.-L. Hodeau, L. Marques, M. Mezouar, and H. Kataura, Phys. Rev. B **74**, 205425 (2006).

[16] S. Kawasaki, T. Hara, T. Yokomae, F. Okino, H. Touhara, H. Kataura, T. Watanuki, and Y. Ohishi, Chem. Phys. Lett. **418**, 260 (2006).

[17] M. Chorro, J. Cambedouzou, A. Iwasiewicz-Wabnig, L. Noé, S. Rols, M. Monthioux, B. Sundqvist, and P. Launois, EPL **79**, 56003 (2007).

[18] P. Zhou, Z. H. Dong, A. M. Rao, and P. C. Eklund, Chem. Phys. Lett. **211**, 337 (1993).

[19] Y. Wang, J. M. Holden, X. X. Bi, and P. C. Eklund, Chem. Phys. Lett. **217**, 413 (1994).

[20] N. Hayazawa, Y. Inouye, Z. Sekkat, and S. Kawata, Chem. Phys. Lett. **335**, 369 (2001).

[21] P. Verma, K. Yamada, H. Watanabe, Y. Inouye, and S. Kawata, Phys. Rev. B **73**, 045416 (2006).

[22] Y. Saito, P. Verma, K. Masui, Y. Inouye, and S. Kawata, J. Raman Spectrosc. **40**, 1434 (2009).

[23] T. Yano, P. Verma, Y. Saito, T. Ichimura, and S. Kawata, Nature Photon. **3**, 473 (2009).

[24] K. Yanagi, Y. Miyata, and H. Kataura, Adv. Mater. **18**, 437 (2006).

[25] K. Akers, K. Fu, P. Zhang, and M. Moskovits, Science **259**, 1152 (1993).

[26] T. Takenobu, T. Takano, M. Shiraishi, Y. Murakami, M. Ata, H. Kataura, Y. Achiba, and Y. Iwasa, Nature Mater. **2**, 683 (2003).

[27] Y. Maniwa, H. Kataura, M. Abe, A. Fujiwara, R. Fujiwara, H. Kira, H. Tou, S. Suzuki, Y. Achiba, E. Nishibori, M. Takata, M. Sakata, and H. Suematsu, J. Phys. Soc. Jpn. **72**, 45 (2003).

[28] K. Matsuda, Y. Maniwa, and H. Kataura, Phys. Rev. B **77**, 075421 (2008).

[29] S. Rols, J. Cambedouzou, M. Chorro, H. Schober, V. Agafonov, P. Launois, V. Davydov, A. V. Rakhmanina, H. Kataura, and J.-L. Sauvajol, Phys. Rev. Lett. **101**, 065507 (2008).

[30] S. Okada, S. Saito, and A. Oshiyama, Phys. Rev. Lett. **86**, 3835 (2001).

[31] M. Yoon, S. Berber, and D. Tomanek, Phys. Rev. B **71**, 155406 (2005).

[32] K. Urita, Y. Sato, K. Suenaga, A. Gloter, A. Hashimoto, M. Ishida, T. Shimada, H. Shinohara, and S. Iijima, Nano Lett. **4**, 2451 (2004).